GRINDING OF MARBLE

by

HANS BRUNNER

Mech.Eng., Swiss Fed. Inst. of Techn., Zürich

(1945)

Submitted in Partial Fulfillment

of the Requirements for the

Degree of Master of Science

at the

Massachusetts Institute of Technology

January 1954

Signature of Author Signature redacted
Department of Mechanical Engineering, Jan. 18, 1954

Certified by Signature redacted
Thesis Supervisor

Accepted by Signature redacted
Chairman, Departmental Committee
on Graduate Students

M E
Thesis
1954

GRINDING OF MARBLE

by

HANS BRUNNER

Mech.Eng., Swiss Fed. Inst. of Techn., Zürich
(1945)

Submitted in Partial Fulfillment
of the Requirements for the
Degree of Master of Science
at the
Massachusetts Institute of Technology
January 1954

Signature of Author _____
Department of Mechanical Engineering, Jan. 18, 1954

Certified by _____
Thesis Supervisor

Accepted by _____
Chairman, Departmental Committee
on Graduate Students

MASS. INST. TECH.
OCT 7 1954
LIBRARY

ABSTRACT

Grinding of Marble

by

Hans Brunner

Submitted to the Department of Mechanical Engineering on January 18, 1954, in partial fulfillment of the requirements for the degree of Master of Science.

In order to obtain information as to the effects of particle size and contacting liquids on the energy required in both comminution grinding and surface grinding of minerals, force measurements in machine shop type surface grinding of marble have been performed.

Preliminary studies revealed extensive cracking along the grain boundaries of minerals due to the anisotropy of the coefficient of thermal expansion. Preliminary microhardness tests showed perfect agreement of the occurrence of fractured impressions in marble with Weibull's statistical theory of brittle fracture. In addition they indicated a reduction of the brittle strength by contacting fluids as well as by residual stresses in the surface.

The amount of brittle fracture in surface grinding, which has a great influence on the energy required, is shown to agree qualitatively with Weibull's theory.

Engg. Lib. M.I.T. Oct. 7, 1954

Inspection of ground surfaces revealed the occurrence of extensive plastic flow in the ground surface and the formation of a severely distorted surface layer. The existence of a huge number of thermal cracks in ground surfaces has been shown by dying and microscopic inspection. These surface cracks enable the grinding fluids to penetrate to the flaws where cracking will start and thus to influence the brittle strength and the grinding energy required. Measurements of the grinding energy and use of various grinding fluids showed that, in addition to the purely physical interaction between marble and fluid, there exists either a physical-chemical or a purely chemical interaction.

The possibility of a reduction of the energy requirements in mineral grinding is of immediate practical interest.

Thesis Supervisor: Milton C. Shaw

Title: Professor of Mechanical Engineering

TABLE OF CONTENTS

		Page
Introduction		1
I.	Properties of Calcite	2
II.	Twinning in Marble	7
III.	Thermal Stresses	12
IV.	Effects of Magnitude of Stressed Volume	18
V.	Polished Surfaces	23
VI.	Ground Surfaces	
	a.) Thermal Cracks	27
	b.) Surface Area	30
	c.) Brittle and Plastic Behaviour	33
	d.) Microscratches	39
VII.	Grinding Chips	41
VIII.	X-Ray Diffraction	45
IX.	Grinding Energy	48
	Conclusions	57
	Bibliography	
	Appendices	

List of Illustrations

		Page
Fig. 1	Structure of calcite	2
2	Slip	4
3	Sliplines	4
4	Etched marble surface	4
5	Mechanism of twinning	5
6	Twinned specimen	5
7	Structure of marble	7
8	Specific energy for twinning	9
9	Intersecting twinband	11
10	Twinbands	11
11	Crack on ground marble surface	13
12	Mechanical hysteresis	16
13	Model for stress calculation	16
14	Surface before microhardness test	18
15	Vickers impressions in marble	18
16	Cracks and sliplines	21
17	Scratches	24
18	Polishing action	26
19	Comparison of crack occurrence with Weibull's statistical theory	21
20	Brittly polished surface	26
21	Inkspot test	27
22	Surface cracks	27
23	Surface cracks	28
24	Surface cracks	28

List of Illustrations - Continued

		Page
Fig. 25	Surface cracks	29
26	Depth of surface cracks	29
27	Surface showing brittle and plastic behavior	33
28	Flaw	33
29	Dry ground surface	35
30	Dry ground surface, etched	35
31	Second surface layer	37
32	Second surface layer	37
33	Second surface layer, etched	38
34	Cross section of second surface layer	38
35	Scratching at different speeds	40
36	Grinding swath	41
37	Marble chip	42
38	Chip	43
39	Chip	43
40	X-Ray technique	45
41	X-Ray diffraction, by etched surface	45
42	X-Ray diffraction, by broken surface	45
43	X-Ray diffraction, by polished surface	46
44	X-Ray diffraction, by polished surface	46
45	X-Ray diffraction, by ground surface	47
46	X-Ray diffraction, by ground surface	47
47	Situation in dry grinding	49
48	Force diagram	51
49	Marble etched in $Ba(NO_3)_2$	56

Acknowledgments

The author wishes to express his gratitude to Professor M. C. Shaw for his numerous and valuable advices.

He also wishes to thank Professor J. T. Norton and Professor P. L. deBruyn of the Metallurgy Department for their valuable help.

The assistance of Professor D. R. Walker, Mr. G. S. Reichenbach, and Mr. M. Hablanian has highly been appreciated and he wants to express his gratitude to them.

INTRODUCTION

In the technology of materials there are four related problems of great interest at the present time.

1. Dependence of the brittle strength on the size of a specimen.

2. Dependence of the yield stress on the size of a specimen.

3. Dependence of the brittle strength on the contacting medium.

4. Dependence of the yield stress on the contacting medium.

To find the dependence of the grinding energy in comminution on the size of the particles produced will be our ultimate interest. However, this requires improved knowledge of the four problems mentioned above. Thus in this thesis necessarily the ambitious attempted has been made to gather more information on the first three of these problems.

The machine shop type of surface grinding is basically similar to comminution grinding and offers the advantage of closely controlled energy input. The complex nature of both kinds of grinding requires the extensive application of simpler auxiliary tests. In addition, the usual lack of familiarity of mechanical engineers (including the author) with minerals required some preliminary studies. Thus the Chapters I to V are an extensive introduction to the main tests, although some new or little known facts are reported in Chapters III, IV, and V.

Marble has been chosen as a representative material from a wide group of minerals showing both plastic and brittle behaviour.

The reader will find many loose ends, but the author considered it as his responsibility to report those too, in oder to facilitate the continuation of the investigation.

I. Properties of Calcite

a.) Structure:

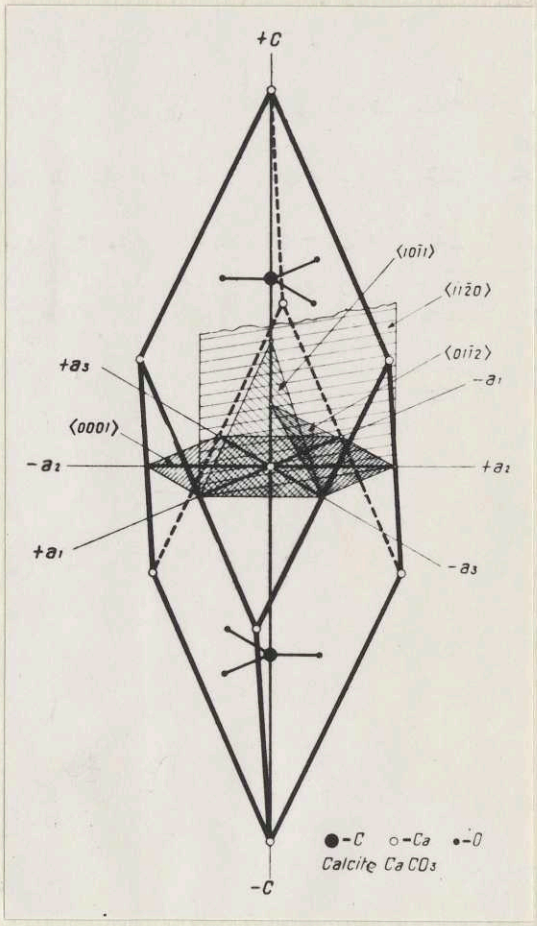

Figure 1
Structure of Calcite

The lattice of calcite is rhombohedral (1), (2). The edges of the elementary rhombohedron (Fig. 1) are 6.2Å long, the lattice constants a and c are 9.95Å and 8.5Å at room temperature. This rhombohedron is formed by the planes ⟨40$\bar{4}$1⟩, ⟨0$\bar{4}$41⟩, and ⟨$\bar{4}$401⟩. The main cleavage planes are ⟨10$\bar{1}$1⟩, ⟨0$\bar{1}$11⟩, and ⟨$\bar{1}$101⟩. These are the planes which are the most densily packed with atoms and have the largest spacing (2) (p. 81). The ⟨11$\bar{2}$0⟩, ⟨1$\bar{2}$10⟩, and ⟨$\bar{2}$110⟩ planes are known as "crack planes" (2).

Calcite is uniaxially anisotropic, all scalar physical constants being different for a and c-directions. The same is true for all crystals with tetragonal or hexagonal lattices. Crystals with orthorhombic, monoclinic, and triclinic lattices have 3 different sets of scalar physical constants.

Only cubic crystals are isotropic. Since the majority of metals have cubic lattices and most of the minerals have non-cubic lattices, anisotropy is the exception with metal crystals, and the rule with mineral crystals. Anistropy is particularly pronounced with calcite. Here for example the coefficients of thermal expansion are:

$$+26.21 \cdot 10^{-10}/^{\circ}C \quad \| \; c \text{ and}$$
$$-5.40 \cdot 10^{-10}/^{\circ}C \quad \perp \; c \qquad (2)$$

However, directional constants (as for example Young's modulus) are anisotropic even for cubic lattice crystals. (11) (Fig.154)

b.) Slip (Translation) in Single Calcite Crystals: Translation is known to occur on the 3 planes $\langle 01\bar{1}2 \rangle$, and in direction $(12\bar{3}1)$. The existance of translation on other planes has not been verified. (38)

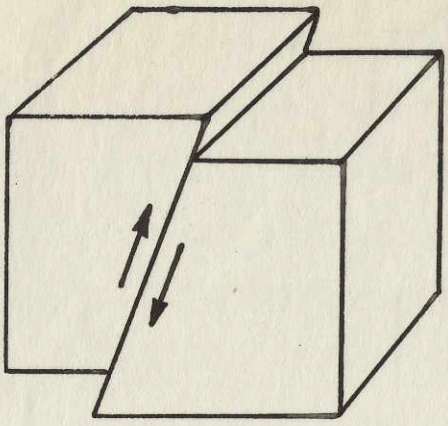

Figure 2
Steps on the Surface
due to slip

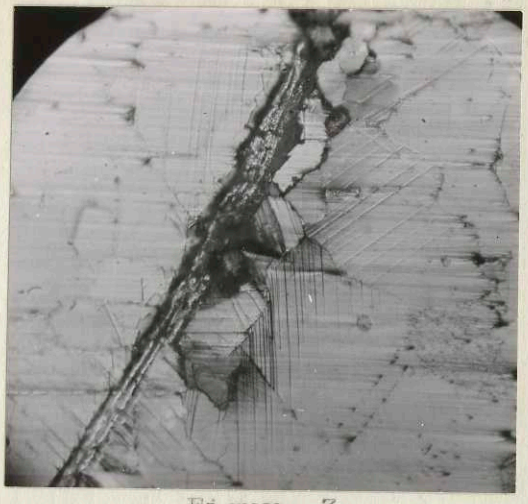

Figure 3
Sliplines in the
Vicinity of a Scratch (60x)

Since a crystal lattice and its directions are not changed by slip, the resulting steps on the surface of a crystal (slip lines, Fig. 2)are the only visible evidences of slip. Polishing of the surface will therefore remove all visual evidence of slip by smoothening out the surface steps. Etching with diluted H_2SO_4 however often makes the sliplines visible again because the remaining lattice distortions are attacked first. (Fig. 4)

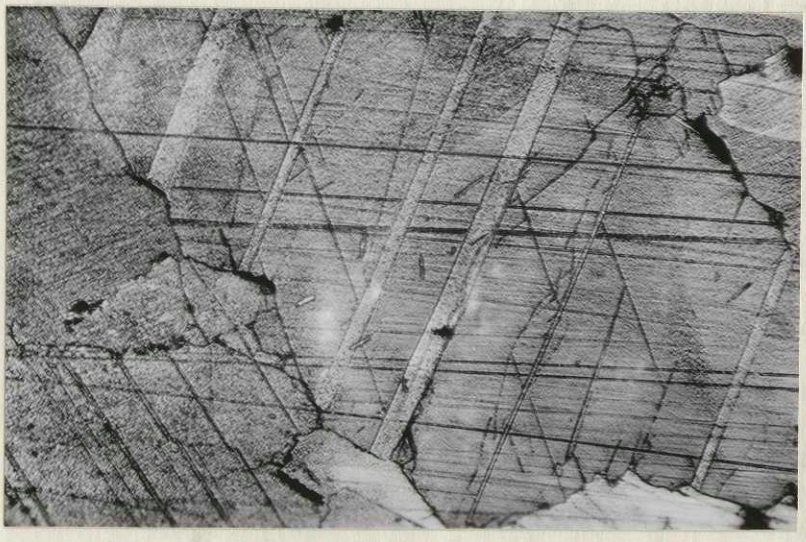

Figure 4
Twins, scratches, sliplines, grainboundaries, and cracks. Marble surface polished and etched with diluted H_2SO_4. (Sliplines, scratches and cracks were not visible before etching, 134x, crossed Nichols and compensator)

c. Twinning in Single Calcite Crystals:

Griggs and Miller (6) found that twinning on the $\langle 01\bar{1}2\rangle$ plane of calcite occurs at about 1/10 of the resolved shear stress required to produce slip, which accounts for the frequent occurrence of twinning in marble.

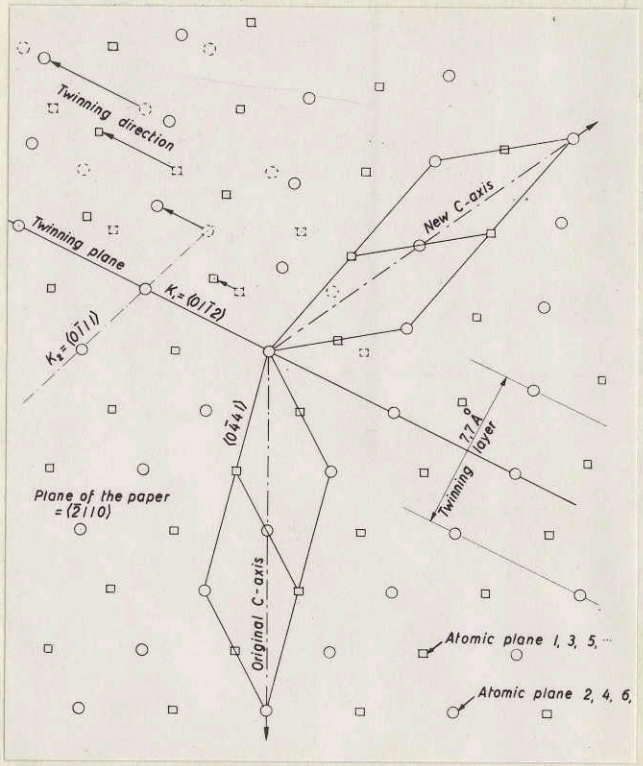

Figure 5
Mechanism of twinning on $\langle 01\bar{1}2\rangle$ plane of calcite (only Ca-atoms are shown)

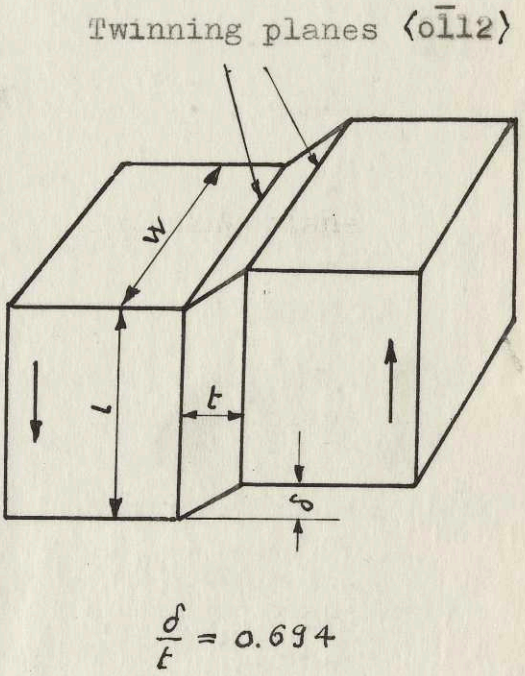

Figure 6
Twinned specimen (2 twinning planes)

Twinning occurs always at constant shear strain (with calcite $\gamma = 0.694$). Therefore the amount of deformation during the twinning process is determined by the width and number of twin bands. It is evident from Fig. 5 that the direction of the optical axis (c-axis) of the twinned crystal differs from the one of the original crystals. Thus

polishing does not remove visible evidence of twinning. This is another reason why many more twin bands than slip lines are visible on a polished and non-etched surface of marble.

Once the twin has been formed its lattice is exactly the same as the lattice of the untwinned crystal except for its different orientation (8). However, Aminoff & Broomé (9) state that the crystal lattice is altered for one atomic layer along the slip planes (twinning layer in Fig. 5). For example α - Zn S (which is cubic) has a twinning layer, which is hexagonal close packed. (so-called "Wurtzit").

The same holds for cobalt, copper, silver, gold, and lead. Kolesnikov (10) proves the same for tin. Since these differences follow from geometrical considerations, the same must be true of calcite. The structure of the twinning layer must generally be a different one, and usually one which is less stable and has a higher energy potential.

II. Twinning in Marble

The marble used consists of an aggregate of calcite crystals. Their average size in the material used for the tests was about 1/100 inch.



Figure 7
Polished marble (66x, crossed nichols and compensator

In any material twins cannot form unless the surrounding grains simultaneously undergo deformation of some kind. Continuous runs of twins are not likely, although they have been observed, since in calcite there are definitely not more than 2 x 3 = 6 planes for mechanical twinning in a crystal, (2), (6), (11), (18). A further restriction is that twinning is possible just in one and not in both directions (compare Fig. 5). Fahrenhorst (11), (Fig. 216), observed continuous runs of twins in Zn. Alternative runs of twins and sliplines can be observed in marble.

Since the shear strain of all twins is equal, it is easy to make a qualitative analysis for the energy V required

to form n twins. Using the nomenclature of Fig. 6, and the letters b, c, d, A for constants, and E and G for the average effective Young's and shear modulus of the crystals affected, we can derive an equation for the energy required to form n twins of equal size by considering:

1. One term which is proportional to the volume of the twins, as observed by Chalmers (12) in single crystals of tin.

   $V_1 = n \cdot t \cdot l \cdot w \cdot A$

2. One term which is proportional to the area of the twinning planes, and which serves to bring the two twinning layers to their higher energy potential (13)

   $V_2 = 2 \cdot n \cdot l \cdot w \cdot b$

3. Two terms which represent the elastic strain energy at the grain boundaries of the twinned crystal. Since the shear strains are the same for all twins, so are the elastic strains at their boundaries. The strain energy thus is proportional to the stressed volumes and to E and G respectively. The stressed volumes are proportional $w \cdot t^2$ and $l \cdot t^2$ respectively. Thus:

   $V_3 = 2 \cdot n \cdot E \cdot w \cdot t^2 \cdot c + 2 \cdot n \cdot G \cdot l \cdot t^2 \cdot d$

These two terms will be zero for a single crystal.

Assuming w = 1, dividing the sum of the energies by the total volume of the twins = $n \cdot l \cdot w \cdot t$, and using new constants B and C, we obtain:

V per unit volume = $A + \frac{1}{t} B + \frac{t}{l} C$

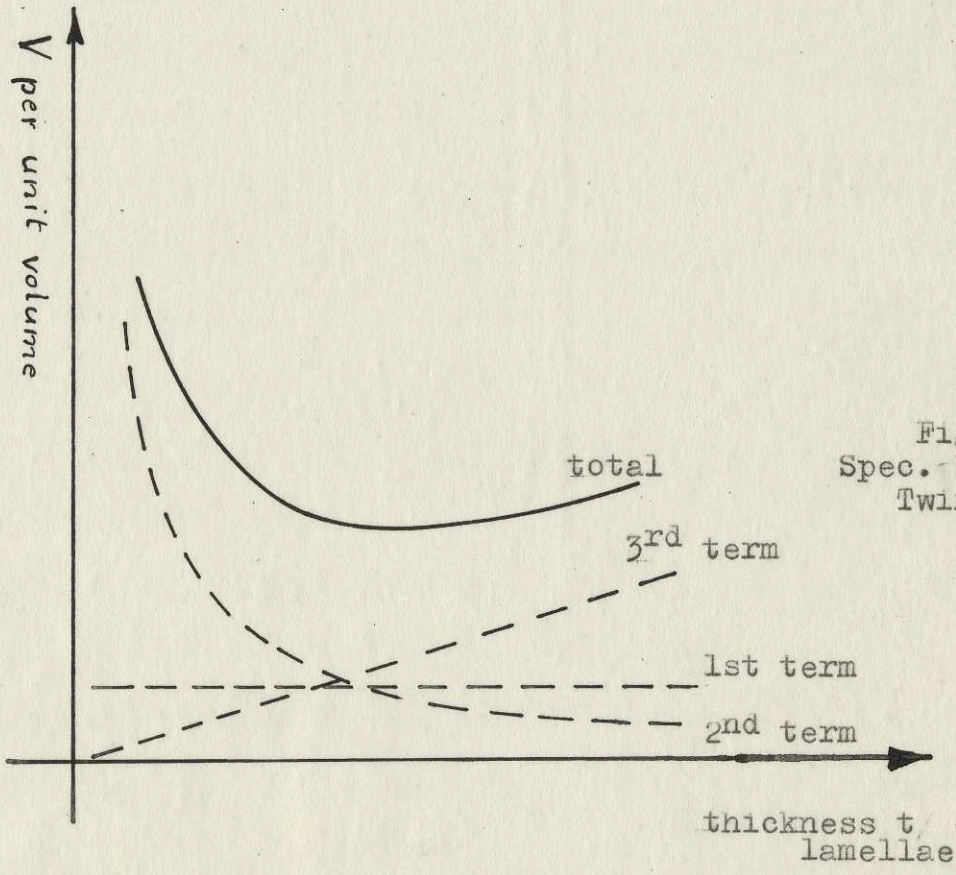

Figure 8
Spec. Energy for Twinning

The energy per unit volume is very high for both very narrow and very wide twin bands, and the formation of twin bands of extremely small or large thicknesses is therefore unlikely. C is actually constant only for small volumes, because the effectiveness of E and G are different for every different

combination of crystals. For this reason the above equation is of more qualitative than quantitative value. However, within a limited section of a grain this equation predicts a fairly equal thickness of the twin bands and this is actually confirmed by observation (Figs. 7, 10, 12). It explains furthermore why microscopic examination with higher resolving power does not disclose any new twins. This is not the case with slip, since it is well known that higher resolving power reveals an increased number of sliplines.

If the formation of a crack at a grain boundary takes less energy than the build-up of elastic stresses (which is especially probably at the ends of the twin bands) then cracking will certainly occur. The lines of intersection of sets of twinning planes may be marked by minute linear cavities (hollow canals), (38), and Fig. 9. A similar observation has been made by Schutze (26) at intersections of slip planes. On the other hand the magnitude of the cracks in Fig. 9 and 10 suggest that some of them existed before the twins were formed, and the problem appears to have often some similarity with the more popular one of which came first: the hen or the egg?

If originally two flaws are accidentally in a favorable position, the residual stresses caused by twinning (and thus the energy requirements) will be at a minimum. Fig. 7 gives numerous examples that these are preferred locations for the formation of twins.

If the ends of a twin band are rounded, the stress concentration and the elastic strain energy will be reduced. Twin bands which tend to be pointed toward their ends can therefore often be observed (for example in Fig. 31), particularly in metals, where cracking requires more energy (Fig. 26 of (7)).



Figure 9
Intersecting twinbands
(360 x, crossed nichols)

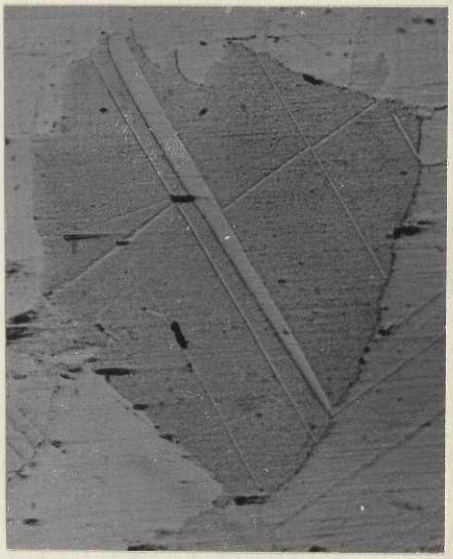

Figure 10
Twinbands, starting at stress concentrations (120 x)

III. Thermal Stresses

a.) "Macroscopic" Thermal Stresses:

"Macroscopic" thermal stresses are due to temperature differences within the specimen. Shaw (14) gave an equation for the surface temperature caused by a friction slider. Regarding the grinding wheel as a friction slider, it can be derived from this equation (Appendix I) that the surface temperature of the specimen is proportional to $\frac{u}{\sqrt{k \cdot \rho \cdot c}}$

where u = grinding energy per unit volume

k = coefficient of thermal conductivity

ρ = density

c = specific heat

The product $(k \cdot \rho \cdot c)$ is at room temperature 10 times smaller for marble than for steel (3). However, the specific energy required to grind marble is about 1/4 of that for steel. Thus, low thermal conductivity and low energy requirement for marble have opposite effects and the resulting surface temperature is about the same for marble as it would be for steel.

The component of the temperature gradient normal to the ground surface is proportional to

$$\frac{u \cdot V}{k} \cdot \sqrt{\frac{d}{R}}$$ (see Appendix II)

where V = table speed

d = depth of cut

R = wheel diameter

The coefficient of thermal conductivity k is about 24 times less for marble than for steel. Thus the temperature

gradient will generally be much higher for marble than for steel. Since the coefficient of thermal expansion is about the same for both materials, much higher thermal strains will result when marble is ground and heat cracks in the surface are to be expected. (Fig. 11)



Figure 11
Crack on ground marble surface, caused by thermal stresses. (1700 x)

b. "Microscopic" Thermal Stresses Due to Anisotropy:

As has been mentioned in a previous section, the coefficients of thermal expansion of calcite parallel and orthogonal to its c-axis are very different. Thus calcite crystals change not only their size but their shape with temperature. Therefore calcitic marble can be stress free only at one temperature. Once plastic flow has occurred, there will be no temperature at which there are no residual stresses. The same is true for all non-cubic metals, as for example, for a wide variety of bearing metals. Boas & Honeycombe (15) found by x-ray back reflection techniques that the lattice distortions of Sn, Cd and Zn accumulate as

the number of thermal cycles is increased. Thus annealing makes matters even worse. They observed that visible slip-lines - mostly near the grain boundaries - are produced by temperature cycles with amplitudes as small as 70°C. In Sn-Sb alloys cracks were formed near the grain boundaries (16). An originally smooth surface warped due to slip and developed a surface roughness of 1/1000 inch.

In calcite anisotropy is much more marked than in any one of these metals. A slight change in temperature certainly promotes crack formation. Howe (17) apparently was the first to realize the importance of this effect in the weathering of rocks. Lord Raleigh (18) made very simple bending tests and investigated the elastic behaviour of marble when it previously had been baked. His test results are extremely important for an understanding of the structure of minerals. He found that the modulus of elasticity of marble dropped to 14% of its original value when it previously had been baked at 336°C. Baking at 336°C caused a permanent elongation of 0.32%. There is no other explanation for these effects than separation of the grain boundaries and consequent reduction of the effective cross section up to more than 86%. As an interesting application I suggest non-destructive testing of building materials by measurement of the sound velocity within the materials.

There is a third confirmation for this theory. Young's modulus of marble varies over a very wide range, and usually

those marbles with the lowest Young's modulus are those with the highest coefficient of thermal expansion, (International critical tables). As mentioned in a previous section calcite crystals grow taller and slimmer with increasing temperatures. The effective coefficient of thermal expansion for marble is an average of the 3 coefficients for calcite and can be calculated as explained by Voigt (20). The calculated value for marble is $3.17 \cdot 10^{-6}$ (Appendix III) and is lower than any of the observed coefficients (3.6 to $16 \cdot 10^{-6}$). If any cracks develop they will form along the contracting sides of the crystals (see Section "crack planes".) As more cracks are formed, the coefficient of thermal expansion for marble will approach calcite's lengthwise coefficient which is $26.2 \cdot 10^{-6}$.

Raleigh (18) observed a tremendous increase in mechanical hysteresis when the marble previously had been baked. (Fig.12) His theory was that hysteresis was caused by friction along the ruptured grain boundaries, but it may just as well be caused by plastic flow of the few intact grains which will be under high stress (Raleigh used a constant load for all tests).

In order to calculate the order of magnitude of these thermal stresses we shall use the model shown in Fig. 13.

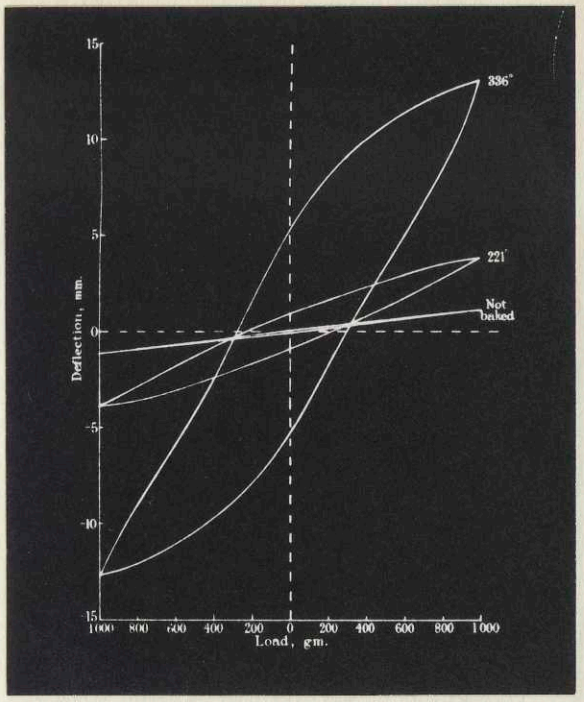

Figure 12
Increase in mechanical hysteresis due to baking (18)

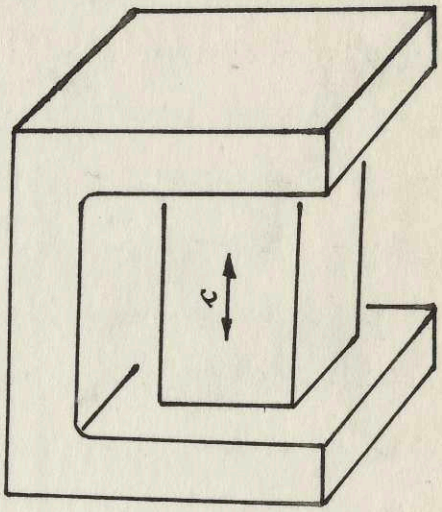

Figure 13
Model for calculation in Appendix IV

We assume a calcite column in a vice of marble, the vice expanding with the observed coefficient of thermal expansion $\alpha = 8.1 \cdot 10^{-6}$ per ^{o}C. This corresponds to the case of crystals with completely cracked boundaries. The calculations, which are included in Appendix IV, indicate a stress $\sigma_z = -145$ psi per ^{o}C.

If we assume the crystal to be completely enclosed in the marble (the grain boundaries being able to transmit tension and the marble having the theoretical coefficient of thermal expansion $\alpha = 3.17.10^{-6}$ per ^{o}C) the calculated stresses will be $\sigma_x = \sigma_y = +76.6$ psi per ^{o}C

and σ_z = -153 psi per °C. The calculations are included in Appendix V. Grigg and Miller (21) found that marble yields at a stress $\sigma_z - \sigma_x = \sigma_z - \sigma_y$ = -17750 psi, if cracking is prevented by hydrostatic pressure. It may be concluded that plastic flow is to be expected with a temperature increase of about $\frac{17750}{153 + 77}$ = 77°C. Since the yield point of a single crystal is much lower than that of an aggregate, first occurrence of plastic flow will be produced by much lower stresses.

A far more intricate calculation of the stresses is given by Laszlo (19). However, the maximum shear stress for cadmium as calculated by Laszlo differs only by 4% from our results for cadmium (Appendix V).

Two important conclusions may now be made:

1. There is hardly a mineral without some grains which are stressed just beyond their yield point and without others which are stressed just beyond their fracture strength.

2. Any theory of brittle fracture which does not consider these high residual stresses cannot be applied to polycrystalline minerals.

IV. Effects of Magnitude of Stressed Volume

The Vicker's microhardness of the marble used was determined with 3 different loads: 4 grams, 9 gr., and 15 gr. The microhardness measured was 188, 166, and 165 kg/mm^2 respectively, with a mean deviation of about ± 16 (20 tests each). Smaller loads could not be used because the load reading mechanism was not accurate enough for this purpose.

Wetting of the surface with an aerosol-water solution has no noticeable influence on the yield stress. Other tests conducted by D. Walker have shown the same to be true with copper and titanium. The average volumes of the impressions were 5.9 μ^3, 24 μ^3, and 52.1 μ^3 respectively, and these are proportional to the stressed volumes, if the yield stress is constant.

The occurrence of fracture showed an important dependence on the volume of the impression. (Figs. 14 and 15)

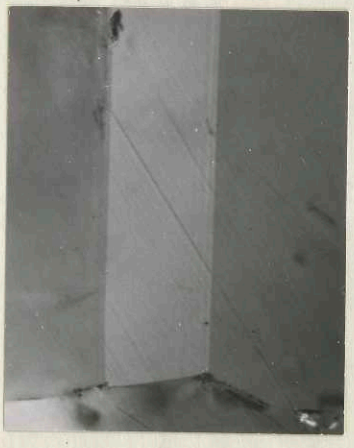

Fig. 14
Marble surface before microhardness test

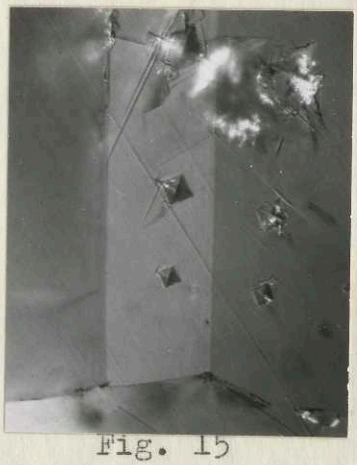

Fig. 15
Vicker's impressions in marble (360 x)

Twenty-two impressions were made with each load used and of these 2, 10, and 17 respectively showed cracks, or, in percentages 9%, 45% and 77%. Because of the limited number of tests these percentages cannot be expected to be the exact probability for the formation of cracks. Somewhat different values may result in exactly the same number of observed fractured impressions. The theory of probability (22), indicates that 11±6%, 45±7%, and 77±6% probably yield exactly the same result for 22 tests. The dependence of the probability of the formation of a crack on the volume of the impression constitutes a definite confirmation of Weibull's statistical theory of brittle fracture (23). This theory states that the probability of finding a stress concentration of sufficient intensity to initiate a crack is $b = 1 - e^{-n VA}$ (Poisson distribution, (22)), where n is the average number of such stress concentrations per unit volume, V is the volume of the impression, and A is a constant, depending on the shape of the impression only. Fig. 19 shows the agreement of the test results with Weibull's equation for this test as well as for two further tests which have been performed. The unknown constant A has the same value for all tests. The magnitude of n will be different for different test conditions. Since we do not know the value of A, it is not possible to determine the absolute magnitude of n. However, it is possible to determine the relative magnitude of n as compared to "standard" test conditions. One of two additional test series

which were made was with exactly the same surface, but freshly polished (one day old). Fractures were observed in 27±9%, 73±9%, and 82±8% of the impressions (11 tests each). This freshly polished surface behaved in a much more brittle manner than the first surface, which had been polished more than a month before the tests. It will later be shown that cracks do not close. Thus it appears that with the other test series relaxation of internal stresses had been more advanced. This serves to illustrate that Weibull's formulation "stress concentrations of sufficient intensity" has to include "sufficient residual stress" as well as "sufficient size of the flaws".

The test results indicate that the number of "stress concentrations of sufficient size" per unit volume was 2 times higher with the freshly polished surface than with the relaxed one. (Compare Fig. 19)

The third test was performed on a "relaxed" surface which was wetted with a 1/10% aerosol solution in distilled water. The percentage of fractured impressions were: 47±8%, 89±5%, and 100±0% respectively. (18 tests). Thus wetting made the surface much more brittle and an increase of n (as compared with a dry surface) by the factor 4.1 is indicated. (Fig. 19) An explanation is offered by Griffith's theory of brittle fracture (24) which states that a crack will propagate when in so doing the accompanying decrease in strain energy

is greater than the resulting increase in surface energy. The increase in surface energy does not only depend on the increase in surface but also on the nature of the adjoining medium too, and is much smaller for a surface contacting an aerosol solution than for a surface contacting air. Thus the strain energy required for propagation of a crack decreases, and now there are 4.1 times as many stress concentrations of "sufficient" size.

Comparing the fairly constant yield stress with the greatly varying crack occurrence it appears that, within the range of volumes stressed, stress concentrations of sufficient size are relatively scarce while inhomogenities as required for the formation of slip are plentiful within the same volume.

A good visual illustration is apparent in Fig. 16, which shows cracks and sliplines in the vicinity of a scratch. This figure shows that there are many more sliplines per unit volume than cracks. It should be noticed that there was no hydrostatic pressure on the surface to prevent cracking when the scratch was made.

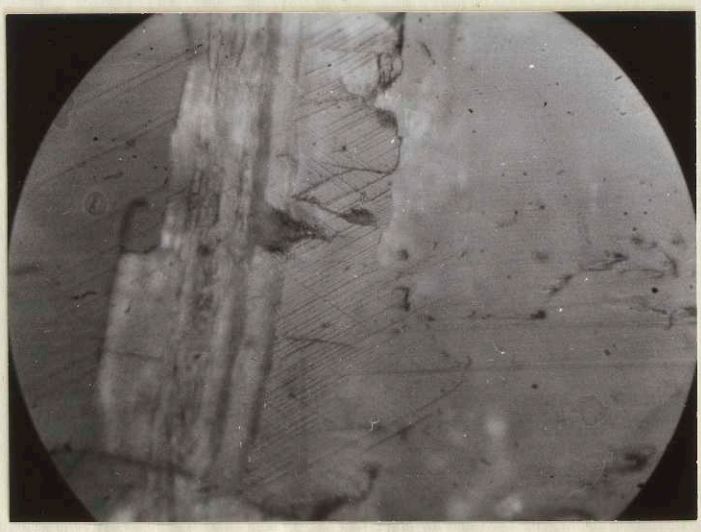

Fig. 16
Cracks and Sliplines in the vicinity of a Scratch (240 x)

80
60
40
20
% FRACTURES
$1-e^{-n_3 \cdot V \cdot A}$
$1-e^{-n_2 V \cdot A}$
$1-e^{-n_1 \cdot V \cdot A}$
$n_1 \cdot A = 0.024 \cdot \mu^{-3}$
$n_2 \cdot A = 0.048\ \mu^{-3}$
$n_3 \cdot A = 0.099\ \mu^{-3}$
10
$100\ \mu^3$
VOLUME V

FIG. 19

As far as the mathematical formulation of the definition "stress concentration of sufficient intensity" is concerned, an additional remark ought to be made.

The size of a crack determines a stress concentration factor which multiplies the stresses resulting from external loads.

On the other hand, residual stresses add to the stresses resulting from external loads. Roš and Eichinger (25), assuming an additive term, have obtained an expression for the dependence of the strength on hydrostatic pressure which for porcelain agreed very well with the results of experiments. Thus the brittle strength is influenced by the size of the cracks, the number of cracks, the stressed volume, the contacting medium, and the residual stresses. Therefore a combination of Griffith's, Weibull's, and Roš's theories on brittle fracture should be made in order to get a useful equation for the brittle strength of crystalline materials.

IV. Polished Surfaces

Polishing of marble was achieved by pressing the surface of the specimen on a rotating horizontal disc which had either a hard (steel) surface or a soft (cloth covered) surface. There were important differences between the surface achieved by these two methods.

a.) Surfaces as Polished with a Soft Disc.

The speed of the disc varied from 200 to 1000 ft/min. Abrasives were Al_2O_3 and tap water for the initial stages of polishing, and diamond 0-2 μ respectively 0- 1/2 μ and kerosene for the final stages. The abrasive grains were embedded in the cloth, and, sliding along the surface, they produced surfaces as shown in all the previously shown photomicrographs except Fig. 11. Surface cracks were not visible except at the grain boundaries. Etching made some additional cracks visible as well as the sliplines (Fig. 4). At the same time scratches became visible which were not visible at all before etching (Fig. 17). It is assumed that these scratches were made in earlier stages of polishing and then plastically filled up in later stages. This filled in material was attacked first by the etching acid. Use of polarized light and crossed nichols, and the transparency of marble allowed microscopic examination to a depth of at least 100 μ, which corresponds approximately to one average grain radius. At this depth often brilliantly reflecting and apparently

cracked surfaces could be observed. Comparison with the grain size suggests that these were grain boundaries.

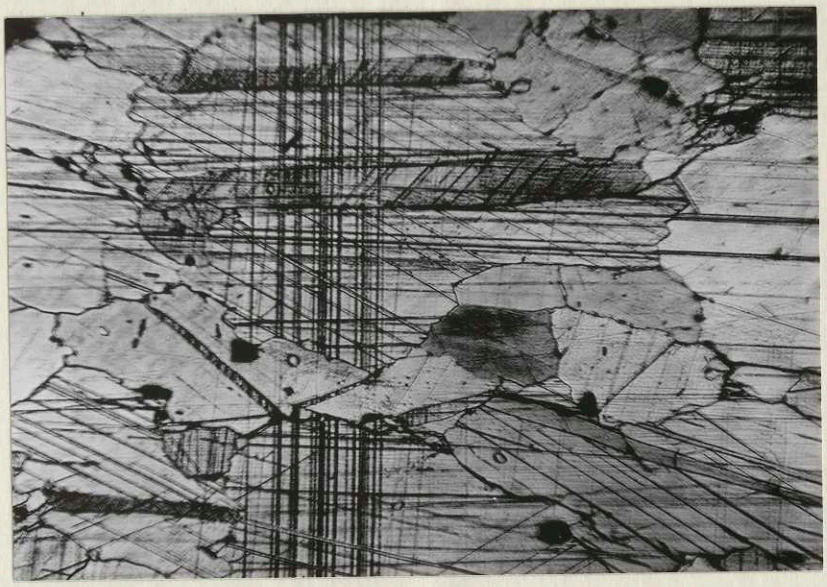

Figure 17
Scratches and slip lines on a marble surface polished on a soft disc and then etched. (70 x)

An interesting detail is that these reflecting cracks were very rare right after polishing and that their number increased for about one hour. A similar observation was made by Lad (27) on polished NaCl surfaces. In our case the possibility was not excluded - although improbable - that there was polishing fluid in the cracks and that the cracks became visible when this fluid evaporated.

Seitz and Read (28) calculated that thermal fluctuations are not sufficient to initiate cracking within a reasonable time. However, they did not consider any residual stresses and their calculations yield a different result if this is done.

Residual stresses up to the so-called theoretical strength were observed on NaCl by photoelastic and x-rays methods by Obreimow (29) and Konobojewski (30). In reviewing the literature one receives the impression that the magnitude of the observed maximum residual stresses depends mainly on the volume checked: the smaller the volume, the higher the observed residual stresses.

If we assume the crack formation to be triggered by thermal fluctuations it follows that cracking is completed within a shorter time at higher temperatures. However, no dependence of the brittle strength on temperature has been observed (31). Then there is no explanation other than that the weakening effect of the cracks is equivalent to the weakening effect of residual stresses. This would be in line with conclusions of a previous chapter. Marble is not a suitable material to check this assumption since its residual stresses are extremely sensitive to temperature changes.

b.) Surfaces as Polished on a Hard Disc.

The speed of the disc was about 200 ft/min. As an abrasive tap water and SiC was used (fineness F/2). In this case the abrasive grains were rolling along the surface and, being able to penetrate into the valleys, they stressed a much larger volume of the marble surface than the sliding abrasives which just smoothened the tips. (Fig. 18). Therefore the marble behaves much more brittle in this case.

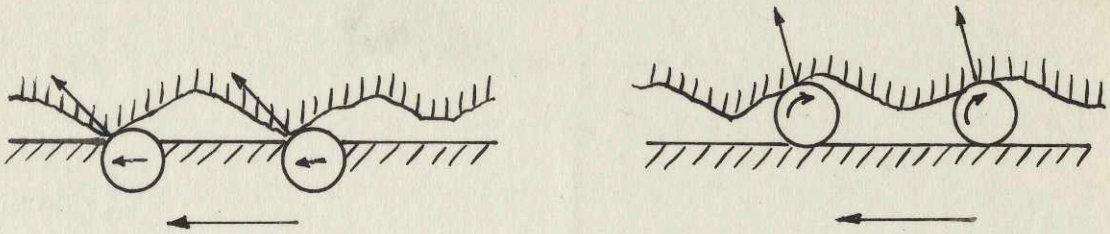

a.) Soft Lap b.) Hard Lap

Fig. 18
Difference in the polishing action of sliding and rolling abrasives.

A marble surface as produced by this method is shown in Fig. 20. There is no visual evidence of plastic flow at all. X-ray diffraction (Chapter VII) will show that lattice distortions occur, indicating increased residual stresses due to polishing.



Fig. 20 (400 x)
Surface as polished with rolling abrasives.

VI. Ground Surfaces

In all of the grinding tests a surface grinder with a 60 grit, H hardness, vetrified bond, Al_2O_3 wheel of 7" diameter was used. The wheel speed was 2000 ft/min, the table speed was 12.2 ft/min and the depth of cut was varied from $1/8 \cdot 10^{-3}$ in to $4 \cdot 10^{-3}$ in.

a.) Thermal Cracks

In all of the ground surfaces, whether they were ground wet or dry, the existence of a huge number of thermal cracks could be shown. A very simple test to show this is the inkspot test (Fig. 21).

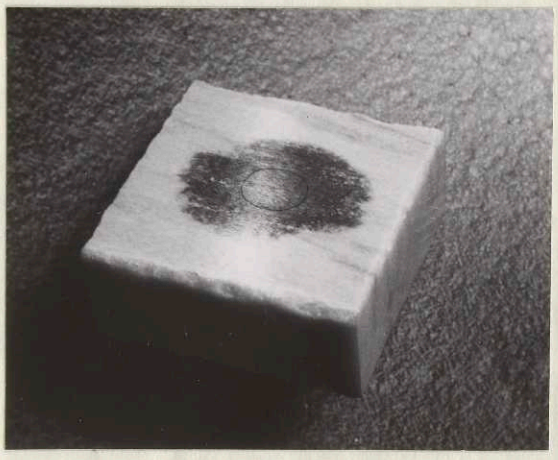

Fig. 21
Inkspot Test

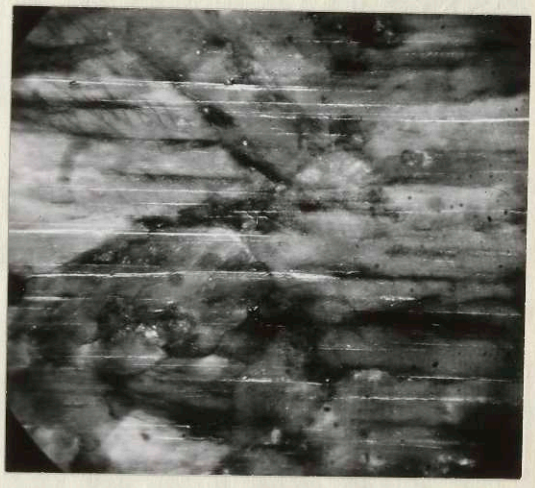

Fig. 22
Cracks in Marble Surface.
Marble dyed with methylenblue
(oblique light, 60 x).

The preferred locations for the cracks were the grain boundaries; the preferred direction was the grinding direction (Fig. 22). Similar cracks could be produced by sweeping a torch over a marble surface. A closer examination (Figs. 23 and 24) shows that from these main cracks shorter cracks branch off approximately orthogonal to the grinding direction.

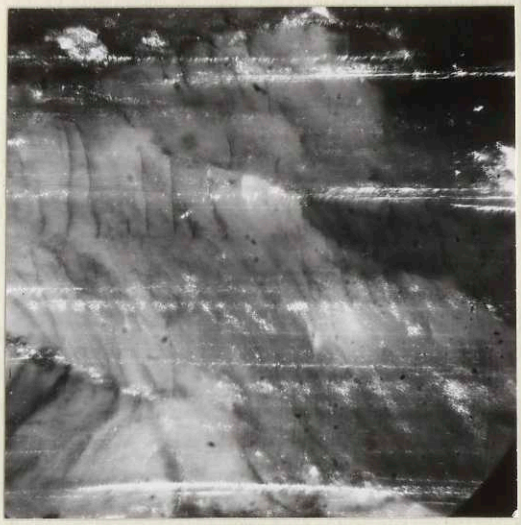

Fig. 23
Cracks in dry ground marble surface,
(oblique light, 240x)



Fig. 24
Cracks in wet ground marble surface.
(oblique light, 240x)

One of these orthogonal cracks was shown in Fig. 11, one of the intersections is shown in Fig. 25.

An estimate (Appendix VI) of the temperature increase at the surface gives us 416°C for a depth of cut of $1/2 \cdot 10^{-3}$ in., and 890°C for a depth of cut of $4 \cdot 10^{-3}$ in., if 40% of the grinding energy is assumed to flow into the specimen in the form of heat. Tests on the percentage of heat flowing into the specimen have not been performed on marble. Since there are no data available, the percentage as found in a previous term paper for steel has been assumed. Measuring the radiation seems to be the only way to get experimental data on the surface temperature. A test procedure to measure radiation with a lead sulfide cell is being developed at the present time by the Metal Cutting Laboratory. Using the same data and the equation for the temperature gradient

as derived in Section IIIa, it follows that the temperature gradient for a depth of cut of $1/2 \cdot 10^{-3}$ in. is just 79% of the temperature gradient corresponding to a depth of cut of $4 \cdot 10^{-3}$ in. Our intuition that finer grinding results in fewer cracks is therefore to some extent justified.



Fig. 25
Intersection of 2 surface cracks (1700x)

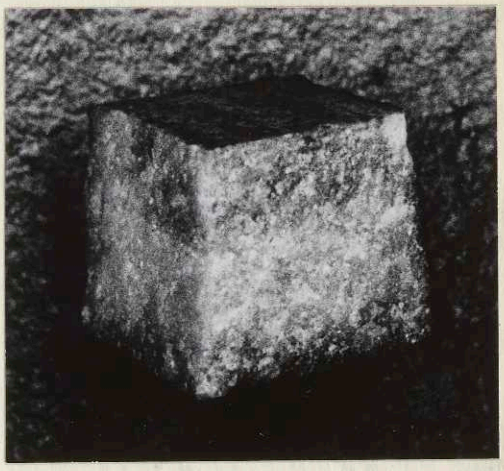

Fig. 26
Depth of penetration of methylenblue into a ground marble surface.

Some of the ground specimens were immersed in a solution of 0.5% methylenblue and 0.05% aerosol (wetting agent), dried, and then broken (Fig. 26). This gives at least a relative measure for the depth of the cracks.

The average depth of the cracks after dry grinding was 8.4 mm (0.33") for both $3/2 \cdot 10^{-3}$ in. and $4 \cdot 10^{-3}$ in depth of cut. Aging of the specimen for 8 days before dying had no noticeable influence on the depth.

Grinding in a solution of 1/10 M $Ba(NO_3)_2$ with a depth of cut of $4 \cdot 10^{-3}$ in. and dying immediately thereafter showed an average depth of the cracks of 2.7 mm. (0.11"). $Ba(NO_3)_2$ solutions appear to react not only physically with marble, but also chemically under certain conditions, as will later be shown. Clogging of the surface cracks is tentatively suggested as an explanation for the fact that the depth of the cracks seemed to be reduced from 8.4 mm to 2.2 mm (respectively from 2.7 to 1.88 mm with the wet ground specimen) when the specimen after grinding was immersed for 8 days in $Ba(NO_3)_2$ solution. An increase of the bending strength of the specimens was not observed.

b.) Surface Area

The surface areas of some representative samples have been measured by adsorbtion of krypton gas at the temperature of liquid nitrogen (33). First 2 samples with surfaces as cut by the diamond saw were measured.

#1:	Volume =	25.0 cm^3
	Apparent surface =	57.5 cm^2
	Measured surface =	16550 cm^2
#2:	Volume:	25.2 cm^3
	Apparent surface =	103.0 cm^2
	Measured surface =	21500 cm^2

Assuming one part of the measured surface being proportional to the apparent surface (surface cracks A cm^2/cm^2) and another part being proportional to the volume (porosity P cm^2/cm^3),

we get 2 equations with the two unknowns A and P.

$$\left| \begin{array}{l} P \times 25.2\ cm^3 + A \times 103\ cm^2 = 21500\ cm^2 \\ P \times 25.0\ cm^3 + A \times 57.5\ cm^2 = 16550\ cm^2 \end{array} \right|$$

$A = 106.8\ cm^2/cm^2$ $\qquad$ $P = 417\ cm^2/cm^3$

This indicates that the surface area of the surface cracks is 106 times as great as the area of the apparent surface.

Taking the depth of the cracks equal 41 mm (as measured by dying), we get an average spacing of the surface cracks = $\frac{2x2x4.1\ mm}{106}$ = 0.155 mm, or approximately equal to the grain size. For a dry ground surface 282 cm^2/cm^2 was the measured value for A. Taking the depth of the cracks equal 8.4 mm (as measured by dying), we obtain an average spacing of the surface cracks = $\frac{2x2x8.4\ mm}{281}$ = 0.12 mm, or again approximately equal to the grain size. A, as measured for a wet ground surface, was 153 cm^2/cm^2. With 2.7 mm for the measured depth of the cracks we get an average spacing of $\frac{2x2x2.7}{152}$ mm = 0.071 mm. Thus there are mor cracks per unit volume for wet grinding, which is another confirmation of the results obtained by microhardness tests.

There are many objections to be made with regard to the reliability of surface measurements by gas adsorbtion. The one most often heard, that the gas does not penetrate to the tips of the cracks, is of little concern, since the molecular diameter of krypton is 4.1 $\mathring{A}$ and the lattice constants of

calcite are about 9Å. A second objection, that only surfaces which are connected with the outer surface are measured, is more justified. But the most serious drawback of this method is that the material had to be cooled down to the temperature of liquid nitrogen (-196°C). This, as explained in a previous chapter, will cause cracking along the grain boundaries and thus permanently increase the surface. This fact was not fully realized when the tests were made, and the above results have to be regarded of value only for comparison.

A powder consisting of cubes of thickness 1/200 of an inch would correspond to a porosity P = 472 cm^2/cm^3. Thus, by comparing with the measured value of P and with the grain size, it can be concluded that a temperature of -196°C results in grain separation of a majority of the grains.

This very serious restriction to the application of the gas adsorbtion method is not realized by most users. For example, the research institutes of the cement industry are widely using the gas adsorbtion method. Oddly enough, the same industry is using the effect of temperature changes as an aid in comminution on a huge scale. So-called air quenching is widely used as an aid not only in crushing but in the fine grinding of clinker too. The effect of air quenching cannot be explained by thermal stresses due to local temperature differences, but only by microscopic thermal stresses due to anisotropy of the crystals.

c.) Brittle and Plastic Behavior

Marble exhibits both plastic and brittle behavior in surface grinding, exactly as it does in polishing. Figure 27 shows a ground surface where marble behaved both ways. It should be noted that even in the area of the surface which appears at first sight rough and dull, the tips are always plastically smoothened.

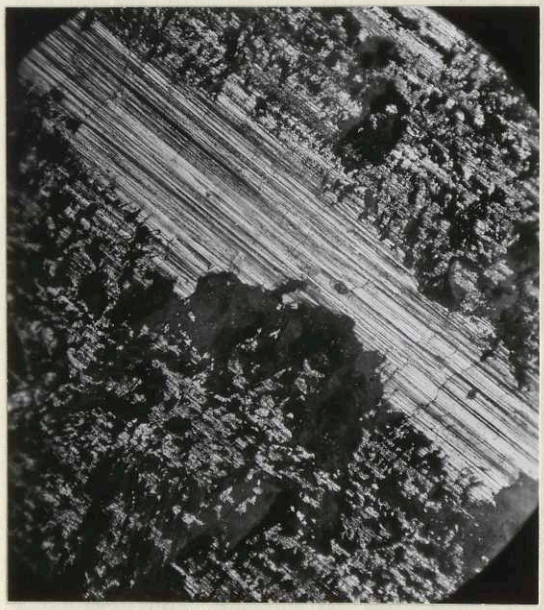

Fig. 27
Completely plastic and partly brittle areas of a ground marble surface (60x).



Fig. 28
Flaw in bottom of pit. (1700x)

Again it is evident that the brittleness of marble is governed by the presence or absence of a "stress concentration of sufficient size" within the stressed volume. The volume of the tips of the surface roughnesses being very small, there is little chance of finding a sufficient stress concentration there, and thus the tips behave generally plastically. Figure 28, showing the bottom of a pit (which has actually

never been touched by the grinding wheel), proves the presence of randomly distributed flaws and indicates that cleavage planes preferably run through these flaws. The ratio tip-surface:pit-surface depends mainly on the ratio brittle-strength: yield-stress. As stated by Becker (4) the yield stress decreases with increasing temperature (corresponding to increased depth of cut). On the other hand the brittle strength is decreased by the application of a grinding fluid (Griffith (24)). In all our experiments the effect of these variables on the amount of pitting as stated has been confirmed. A decrease of the yield stress due to the physical action of contacting fluids has repeatedly been reported for various materials (21). If this holds true then it seems to be of secondary importance in the case of grinding of marble.

Glossy areas of the ground marble surface resemble a ground metal surface (Fig. 29). Higher power magnifications are given in Figs. 11 and 25. The depth of cut was $4 \cdot 10^{-3}$ for all 3 photomicrographs. Finer grinding resulted in smoother grinding marks.



Fig. 29
Dry ground marble surface
(240x)

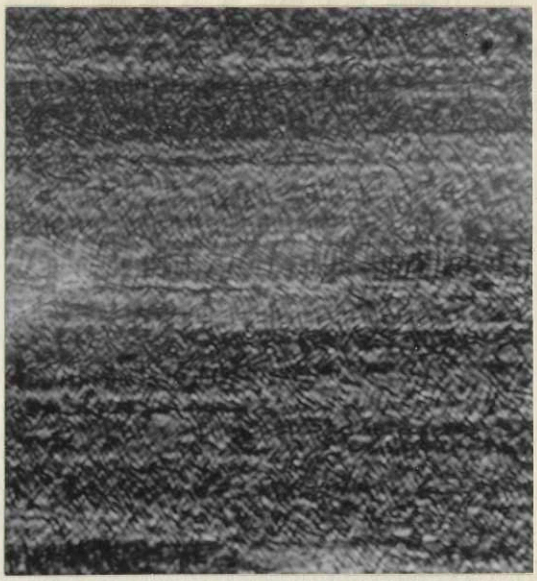

Fig. 30
Dry ground marble surface, etched with diluted H_2SO_4
(1000x, crossed nicols)

All marble surfaces with grinding marks appeared foggy when microscopically inspected with polarized light and crossed nicols. The grain boundaries were diffuse, contrasting very much with the clear appearance and well defined grain boundaries of crushed crystals.

Etching with diluted H_2SO_4 forms numerous etch pits. The orientation of these etch pits is determined by the orientation of the crystal lattice (2). Thus variations in the orientation of the etch pits on a single crystal reveal lattice distortions, in our case obviously caused by plastic flow. Figure 30 shows varying orientations of the etch pits within the area of a single crystal of the ground marble surface, and thus proves the presence of severe lattice dis-

tortions. When the nicols were rotated, local parts of the light strips in Fig. 30 moved sidewise.

The microhardness of this top surface layer was 240, 229, and 219 for 4 gr, 9 gr, and 15 gr load respectively, with a mean deviation of the hardness of about ±25. The volumes of the impressions were 4.1 u^3, 14.9 u^3, and 34.1 u^3, and 0%, 10%, and 33% of the impressions respectively showed cracks. (Compare Fig. 19) This indicates that the average number of "stress concentrations of sufficient size" per unit volume must be only 45% of the corresponding number in a polished surface. The appearance of the impressions was different too. Their vicinity showed a network of dark lines similar to that which will later be seen on the surface of the grinding chips.

If the top surface layer shown in Figs. 29 and 30 is removed by polishing then another surface layer can be seen (Figs. 31 and 32). This second layer is distinguished by extensive deformations and thus cannot be identical with the original marble. It cannot be identical with the previously described top layer either since there the etch pit pattern (Fig. 30) was symmetrical with respect to the grinding direction which is not so for the second layer (Figs. 31 and 33).



Fig. 31
Second surface layer
(630x, crossed nicols)

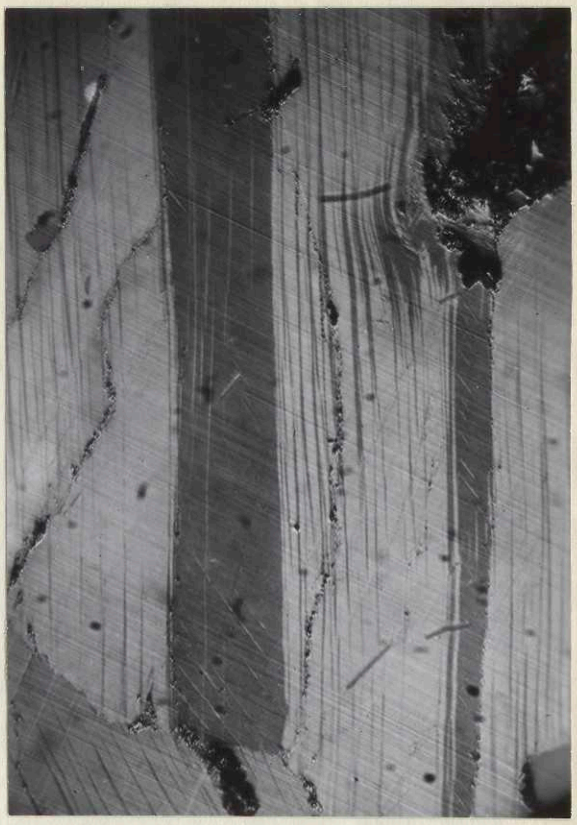

Fig. 32
Second surface layer
(390x, crossed nicols)

We will notice that most of the twins and sliplines are smoothly bent. Since certainly not more than six crystallographic planes of the crystal lattice are available for twinning, this means that the entire crystal lattice is elastically bent. The estimated strain as read from the most severely bent parts of Fig. 32 is up to 2%, or of the same order of magnitude as that of the best steel at the yield point!



Fig. 33
Second surface layer, etched
(630x)



Fig. 34
Cross section of second
surface layer
(130x, crossed nicols)

Microscopic inspection with crossed nicols of the fractured sides of the ground specimen of Fig. 26 revealed the cross section of the second surface layer (Fig. 34). For a depth of cut of $3/2 \cdot 10^{-3}$ in. their thickness varied from 1 to $5 \cdot 10^{-3}$ in., for a depth of cut of $4 \cdot 10^{-3}$ in. the thickness of this layer was less uniform and the average about $3 \cdot 10^{-3}$ in. For comparison the mean peak-valley distance may be of interest. This distance was about $1/4 \cdot 10^{-3}$ in., corresponding to a surface roughness of 45 RMS μ in. It may be concluded that each pass of the grinding wheel forms a new deformed surface

layer, and that the majority of the removed material has properties differing from those of the original marble.

d. Microscratch Technique

As to the effect of the magnitude of the stressed volume on the yield stress a definite trend has been indicated by the results of the microhardness tests, but not enough to justify further conclusions.

As stated by Becker (4) thermal fluctuations trigger the formation of slip. Therefore not only the magnitude of the stressed volume, but the duration of the load too have an influence on the formation of sliplines. An easy and accurate way to change the time factor is to make a scratch and to vary the speed of scratching (Fig. 35). The vickers pyramid of the microhardness tester was useful for some qualitative tests. A load of 9 grams produced on a ground surface a groove of 10.3 μ width. In a representative test on each side of the groove there was a plastically deformed zone 5 μ wide. Increasing the scratch speed by about a factor of ten (estimated) produced a groove of approximately the same width, but the plastically deformed zones were just 2 μ wide. The sliplines will be visible on the photomicrographs and can statistically be evaluated. The only refinement necessary is a device to produce a constant scratching speed.

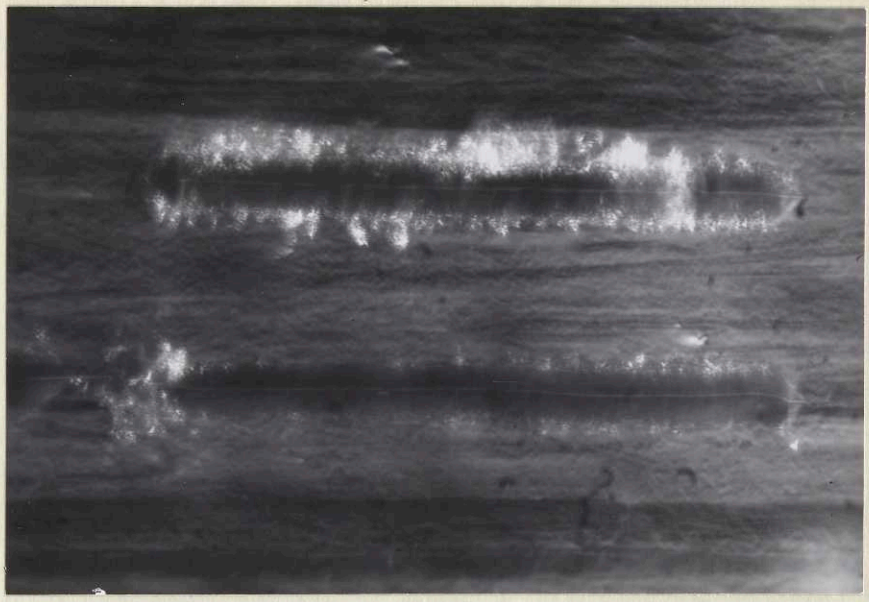

Fig. 35
Scratching of the surface at different speeds
(630x, crossed nicols and comparator)

Microscratch technique on transparent minerals without double refraction, combined with microscopic examination in polarized light, and possibly combined with very little etching, promises to be an extremely useful tool to obtain further information. It approaches very closely the conditions in surface grinding, but the test conditions are much easier to control than in actual grinding.

VII. The Grinding Chips

The particles removed from the marble surface had partly the appearance of a brittly fractured mineral and partly that of a plastically deformed metal (as grinding chips from metals) Fig. 36 represents a sample of grinding swatch as it appears under the microscope. The brittly fractured particles could not be focused, because of their greater vertical extension. Thus they appear diffuse in the photomicrographs.

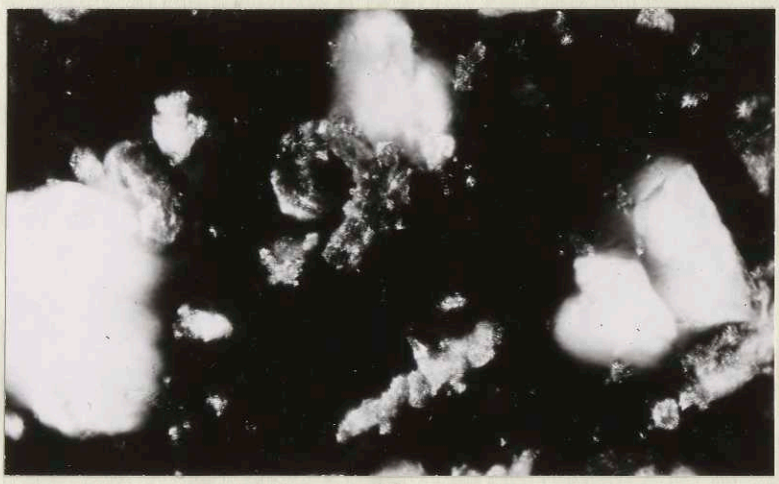

Fig. 36
Particles removed by grinding
(400x, crossed nicols)

Larger chips often had one smooth and one dented side exactly as do chips from metal cutting. (Fig. 37).



Fig. 37
Marble chip (400x, crossed nicols)

Although about half of the chips from dry grinding had fractured surfaces, often literally no fractured surface was visible on the ground surface. This paradox can easily be explained by assuming that the "tails" of the chip always behaved plastically, while the thick ends of the chips often broke off brittly due to their larger stressed volumes. The size of the chips is, of course, not uniform and the smallest chips behave completely plastically.



Fig. 38
Smooth chip
(400x, crossed nicols)



Fig. 39
Usual appearance of chips
(1000x, crossed nicols)

Figure 38 shows a chip with approximately parallel translation planes. This suggests that this chip as well as the one in Fig. 37 consists of a single crystal, although a distorted one. However, a chip with such smooth surfaces as in Fig. 38 was a rare exception. The great majority of chips looked as shown in Fig. 39. The pattern of irregular dark lines on the crystal surface is very characteristic not only for chip surfaces, but for the plastically deformed vicinity of the impressions of the microhardness tester in a ground surface too. The vicinity of a scratch as produced by a vickers pyramid on a ground surface has exactly the same appearance, and this zone cannot be darkened by

rotating the nicols (Fig. 35). On the other hand the vicinity of a scratch on a polished surface behaves optically the same way as the crystal, and the sliplines are straight as shown in Figs. (3) and (16).

Irregular dark lines are characteristic of both grinding chips and ground and subsequently deformed surface. Peyché (37) writes that "a rapidly frozen glass appears to be truly plastic (checked with an electron microscope), a property it loses on annealing". It seems not impossible that the top layer of a ground surface as well as part of the grinding chips consist of a rapidly frozen Beilby layer. An inspection of the chip surface with an electron microscope and determination of the chip structure by more precise methods appear to be of prime interest.

To complete the bibliography it may be mentioned that Wick and Carter (34) found that powdered calcite was discolored a slate gray under the influence of high voltage cathode rays. This is generally considered as an indication of high residual stresses (8).

VIII. X-Ray Diffraction

Chromium radiation and a voltage of 35000 V was used. The method applied is schematically shown in Fig. 40. The diameter of the x-ray beam was approximately 1 mm.

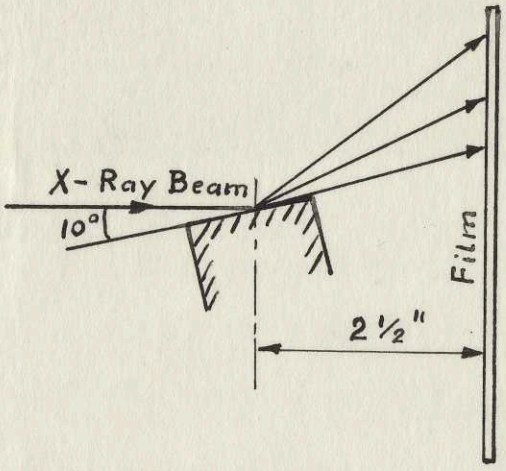

Fig. 40
Method applied



Fig. 41
Marble surface etched in H_2SO_4

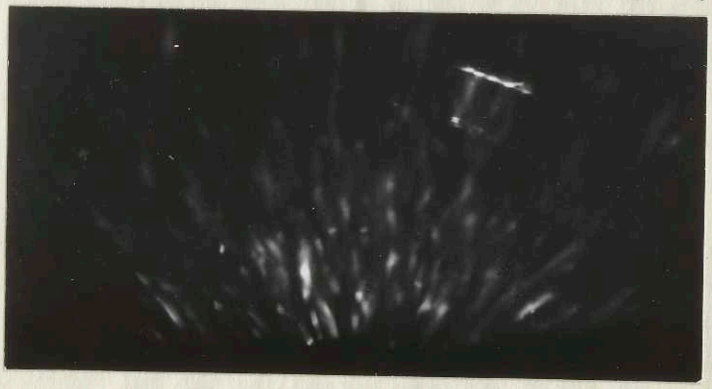

Fig. 42
Broken surface



Fig. 43
Surface polished with rolling abrasives

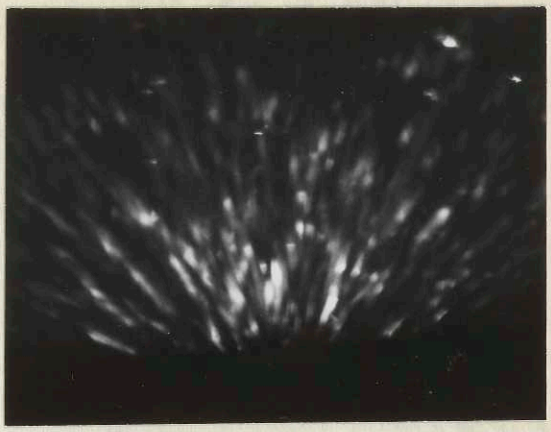

Fig. 44
Surface polished with sliding abrasives

Comparison of Fig. 42 with Fig. 41 shows that an apparently brittle rupture involves marked residual stresses. Polished surfaces show, as expected, increased evidences of lattice distortions. However, there is no noticeable difference between the diffraction patterns of specimens polished with rolling and of those polished with sliding abrasives (Figs. 43 and 44). The particular differences are restricted to a surface layer of unsufficient thickness to show up in x-ray diffraction patterns.

Davis and Stempel (35) found that split calcite single crystals produced a narrower maximum of the reflected x-rays than did polished surfaces. This agrees with the present test results.



Fig. 45
Wet ground marble

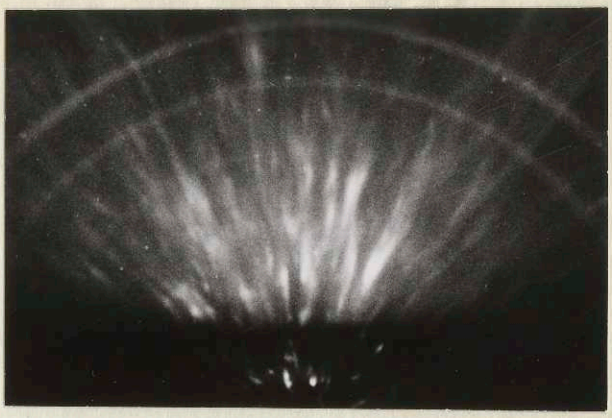

Fig. 46
Dry ground marble

The broadening of the dots in Figs. 45 and 46 indicates extremely severe lattice distortions in the ground marble surface, thus confirming our conclusions from Fig. 32.

Broadening sometimes is caused by the breaking up of original crystals into crystallites small enough to produce the effect of particle size broadening. However, Rosenthal and Kaufman (36) found, that "the x-ray line broadening of the plastically deformed marble (compression test) is due very little to the particle size effect. The inference is that the observed line broadening is caused by microstresses which are relaxed when the specimen is reduced below a certain critical size. In the present case the domain has been found to be around 3 μ ...". This incidentally corresponds to the width of the twins in Fig. 31.

IX. Grinding Energy

The energy required per unit volume of material removed is of prime interest in comminution for economical reasons, for dimensioning of grinding mills and rock drills, and for theoretical reasons. Although surface grinding is a very complex process, this process appears to be simple as compared to the process of comminution, and valuable clues as how to proceed in comminution may be obtained in surface grinding.

As mentioned in Chapter VII, dry grinding of marble on a surface grinder actually involves three different materials, namely:

1.) Top surface layer of so far unknown thickness and structure. This layer is both harder and tougher than marble.

2.) Deformed surface layer (with an average thickness of $1.5 \cdot 10^{-3}$ in. for a representative case). The hardness of this layer is the same as for marble, but the brittle strength is much lower.

3.) Marble. Each one of these layers may behave either brittly or plastically, depending on the actual depth of cut (Fig. 47) within the respective layer and on the contacting medium, to name only the most important factors.

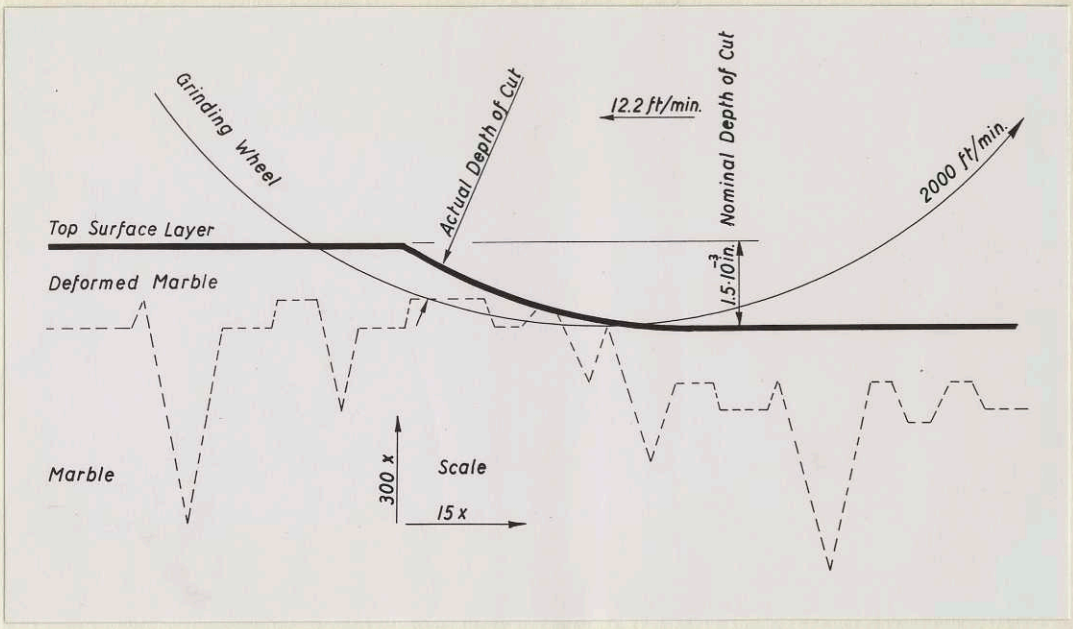

Fig. 47
Situation in dry surface grinding (schematically)

Figure 47 shows schematically the situation in dry grinding of marble with a wheel depth of cut of 1 1/2·10^{-3} in. Inspection of the grinding swath shows that some of the material removed always breaks off brittly. As has previously been shown the statistical chances of the occurrence of brittle fracture increase with increasing stressed volumes. Figure 47 shows that the actual depth of cut, and thus the stressed volume, is a maximum near the old surface. We may conclude that the brittly removed particles mostly originated near the old surface. The new surface actually shows no evidence of brittle fracture in dry grinding.

In wet grinding often the entire thickness removed behaves brittly, and in this case the new surface produced has a dull appearance. Microscopic inspection shows that plastic flow

then is restricted to the tips of the surface roughness. Sometimes the depth of brittly removed material is exactly equal to the thickness of the removed layer and then little differences in the grinding conditions are apt to change the appearance of the produced surface locally. Glossy strips, such as those in Figs. 27 and 48 indicate no brittle fracture and appear most often near the center line of the specimen, thus indicating that temperature is an important factor (Fig. 48 is a rather rare specimen with respect to the location of the glossy strips). Whenever glossy areas showed up on the ground surface, an increase of the grinding forces can be observed. The force diagram in Fig. 48 shows an increase of 5%, and this indicates that the increase would be 20% if the whole surface were glossy. Since the thickness of the plastically removed layer never is as large as the total thickness of the removed layer, it must be concluded that the energy per unit volume required to plastically remove marble is much more than 20% higher than the energy per unit volume required to remove marble in a brittle manner.

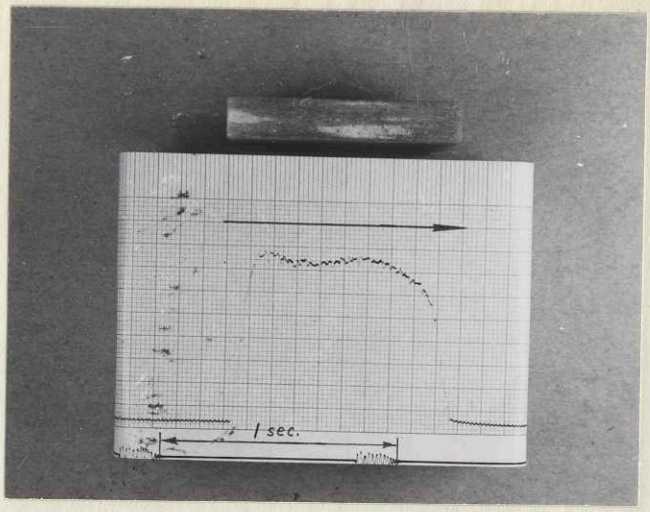

Fig. 48
Force diagram

In Dry grinding with a depth of cut of $1.5 \cdot 10^{-3}$ in. the force exerted by a grinding wheel of 3/8" width on the surface is 33.7 lbs., as has been measured. The horizontal component is just 8.5 lbs. This corresponds to an average normal pressure on the contact surface (in Fig. 47) of 880 PSI. The surface cracks have been omitted in Fig. 47, because their depth would be magnified to one yard! It would be hard to understand how such low compressive stresses on the surface can have a significant influence on the propagation of the tips of the cracks. This is one of the reasons which lead us to the conclusion that the surface cracks must be propagated by thermal stresses due to local temperature differences, rather than by external loads. This also explains why, as previously mentioned, the depth of the cracks is reduced to 1/3 of their length after dry grinding by the application of a grinding fluid (cooling

action). As previously mentioned the surface cracks are very closely spaced. In Fig. 47 there would be up to 100 per inch surface length. The weakest points in the whole crack system obviously are intersections of horizontal flaws (Fig. 28), or cracked horizontal grain boundaries with the surface cracks, which are essentially vertical. Since the depth of the surface cracks is seventy times larger than the depth of the material removed with one pass of the grinding wheel, grinding fluids have plenty of time to penetrate to the flaws before grinding has proceeded to them. In order to determine the magnitude of the effect of grinding fluids, force measurements in surface grinding have been made and the energy per unit volume removed has been calculated for various fluids and depths of cut.

For the force measurements a resistance strain gage dynamometer as described by Marshall and Shaw (39) was used. The dynamometer was carefully waterproofed to prevent any changes of the resistence due to humidity.

Application of various aquos solutions resulted in a very marked decrease of the energy requirements. The results were:

Contacting Medium	Surface Tension T liquid-air dynes/cm (measured)	Approx. Ph	Depth of Cut $4 \cdot 10^{-3}$ in Spec.Energy in lb/in^3	% of dry energy	$1/2 \cdot 10^{-3}$ in Spec.Energy in lbs/in^3	% of dry energy
Air	-	-	$1.7 \cdot 10^6$	100	$3.8 \cdot 10^6$	100
H_2O	71.4 (exact value 73.0)	5	$1.3 \cdot 10^6$	76	$2.35 \cdot 10^6$	62
Tap water	72.6	5	$1.1 \cdot 10^6$	65	$2.2 \cdot 10^6$	58
Na_2CO_3 1/40 M	68.3	10	$1.12 \cdot 10^6$	66	$2.15 \cdot 10^6$	57
Na_2CO_3 1/10 M	61.0	10	$1.16 \cdot 10^6$	68	$2.25 \cdot 10^6$	59
$Ca(NO_3)_2$ 1/10 M	67.5	4	$1.20 \cdot 10^6$	71	$2.25 \cdot 10^6$	59
$Ba(NO_3)_2$ 1/10 M	69.9	4	$0.82 \cdot 10^6$	48	$2.25 \cdot 10^6$	59
$NaNO_3$ 1/10 M	68.5	4	$1.09 \cdot 10^6$	64	$2.20 \cdot 10^6$	58
$NaNO_3$ 1 M	56.9	4	$0.99 \cdot 10^6$	58	$2.00 \cdot 10^6$	53
Aersol 1/10 %	33.3	5	$1.09 \cdot 10^6$	64	$2.15 \cdot 10^6$	57
Aerosol 1 %	28.9	5	$1.11 \cdot 10^6$	65	$2.14 \cdot 10^6$	56

Both these test results and visual observation indicate increased brittleness (decreased brittle strength) when marble contacts a fluid. This agrees with the results of the previously mentioned microhardness tests as well as with Griffith's criterion for brittle strength.

$$\sigma = \sqrt{\frac{E \cdot T}{2 \cdot a}}$$ where

E = Young's modulus

T = Surface tension marble - liquid

2a = crack length

σ = brittle strength

Since the surface tension marble-liquid is generally lower than the surface tension marble-air, Griffith's criterion gives a satisfactory explanation for the effect of fluids in general.

However, although we do not know the surface tensions of marble with the various fluids, it appears that the differences in efficiency among the fluids cannot be explained by Griffith's equation alone, inasmuch as different energies were obtained with fluids having the same surface tension. In addition to the physical interaction there must be a physical-chemical or chemical interaction at the tips of the flaws.

In recent years many investigators have found that contacting fluids can alter the stress-strain curve of both metals and minerals (21), (40), a fact which is not yet fully understood.

Thus it might be possible that not only the surface tension T in Griffith's equation, but also Young's modulus E is changed by contacting fluids. Griffith's equation would be a poor starting point for investigations in this direction because this equation is based on Hooke's law. But it is interesting to recall an earlier paper of Rehbinder (41) which reports a significant increase of the mechanical hystersis in calcite due to the interaction with oleic acid. This, as observed by Lord Raleigh, corresponds to a decrease of the apparent Young's modulus (Fig. 12).

A more recent paper of Rehbinder (32) states that the wedging pressure of the fluids in the cracks is the important factor. The magnitude of this wedging pressure P is

$$P = 2 \times \frac{(T_{23} - T_{13})}{h}, \quad \text{where} \quad T_{23} - T_{13} \geq T_{12}$$

and: T_{12} = surface tension liquid-air

T_{13} = " " solid-liquid

T_{23} = " " solid-air

h = width of the crack

Purely chemical interaction between marble and grinding fluid would be a third explanation. A $\frac{1}{10}$ M $Ba(NO_3)_2$ solution, which was the top performer among the fluids tested, actually reacts chemically with marble, at least when the crystal lattice is distorted. Figure 49 shows a dry ground surface (as in Fig. 29), which had been etched in the $Ba(NO_3)_2$ solution for eight days.



Fig. 49
Marble surface etched in $Ba(NO_3)_2$ solution (1000x)

Conclusions

The tests have shown that both plastic flow and brittle fracture occur in all grinding or polishing operations of marble except for soft lap which may occur purely plastically. The amount of brittle fracture has been shown to be determined mainly by Weibull's statistical theory of brittle fracture, that is, mainly by the size of the particles removed.

In the final chapter it has been shown that plastic removal of particles requires more energy than brittle removal. Thus Weibull's theory must have an important part in the prediction of grinding energies of minerals and it predicts increasing energy with decreasing particle size, which is indeed a well known fact.

Since it has been shown that a huge number of surface cracks of great depth result from surface grinding, grinding fluids must have a good chance to penetrate to the cracks where fracture will start and thus to influence the stability of the cracks and the occurrence of brittle fracture.

It is a well known fact that the surface tension of a solid contacting a fluid is always less than the surface tension of the same solid contacting air. Thus the brittle strength of a solid contacting a fluid is less than the brittle strength of a solid contacting air, according to Griffith's criterion for brittle strength and as confirmed by our tests. But, to explain the difference of the effects of fluids with the same surface tension, we have to assume the existence either of a physical-chemical interaction, or

of a purely chemical interaction, or both, in addition to the purely physical interaction at the surface. However, the test series has to be extended in order to reveal the exact nature of this interaction.

From the practical point of view the confirmation of the possibility of great economic savings in comminution and rock drilling by suitable choice of aqueous solutions will be of immediate interest.

The tests have shown that it is impossible to achieve purely plastic removal of marble with the surface grinder used. Greatly varying brittleness is a disturbing factor which ~~of dependence~~ the dependence of does not allow exact conclusions concerning the yield stress on the size of the particles removed.

Bibliography

(1) A. Johnsen, "Die Massengitterdes Kalkspats", Physikalische Zeitschrift, Vol. 15, 1914, p. 713.

(2) P. Niggli, "Lehrbuch der Mineralogie, II Spezielle Mineralogie", Berlin 1926, p. 76.

(3) International Critical Tables, "Nat. Research Council", New York 1930.

(4) R. Becker, Physikalische Zeitschrift, Vol. 26, 1925, p. 919.

(5) E. Orowan, Zeitschrift für Physik, Vol. 89, 1934, p. 605.

(6) D. Griggs, W. Miller, "Deformation of Yule Marble", Geol. Soc. of America, Bulletin, Vol. 62, 1951, p. 853.

(7) C. Barrett, "Structure of Metals", New York 1943

(8) K. Przibram, "Verfärbung von Kalkspatzwillingen", Zeitschrift fur Physik, Vol. 69, 1931, p. 403.

(9) C. Aminoff, B. Broomé, "Strukturtheoretische Studien über Zwillinge" Zeitschrift für Kristallographie, Vol. 80, 1931, p. 355.

(10) G. Kolesnikow, "Geometrie mechanischer Zwillingsbildung von Zinn und Zink", Physikalische Zeitschrift der Sowjetunion, Vol. 4, 1933, p. 651.

(11) E. Schmid, W. Boas, "Kristallplastizität", Berlin, 1935.

(12) B. Chalmers, "The Twinning of Single Crystals of Tin", Proc. Phys. Soc., (London), Vol. 47, 1935, p. 733.

(13) N. Davidson, A. Kolesnihov, K. Fedorov, Journal Exptl. Theoret. Physik, Vol. 3, 1933, p. 350.

(14) M. Shaw, "Metal Cutting Principles", M.I.T., 1952

(15) W. Boas, R. Honeycombe, Nature, Vol. 154, 1944, p. 338.

(16) W. Boas, R. Honeycombe, J. Inst. Metals, Vol. 73, 1947 p. 433.

(17) I. Howe, "The Geology of Building Stones", London 1910, p. 342.

(18) Lord Raleigh, Proc. Royal Soc. A., Vol. 144, 1934, p. 266.

(19) F. László, J. Iron Steel Inst., Vol. 150, 1944, p. 183.

(20) W. Voigt, "Lehrbuch der Kristallphysik"

(21) J. Handin, "An Application of High Pressure in Geophysics: Experimental Rock Deformation", Trans. ASMA, Vol. 75, 1953, p. 315.

(22) W. Feller, "An Introduction to the Probability Theory and Its Applications", Vol. I, New York 1951, p. 142.

(23) W. Weibull, "Investigations into Strength Properties of Brittle Materials", Proc. Ing. Vetenkaps Akademien (Stockholm), No. 151, 1939.

(24) A. Griffith, "The Phenomena of Rupture and Flow in Solids", Phil. Trans., Vol. 221, 1921, p. 163.

(25) M. Roš and E. Eichinger, "Versuche zur Klärung der Frage der Bruch-gefahr nichtmetallischer Stoffe", Eidg. Materialprüfunganstalt Zürich", Diskussionbericht No. 28, 1928.

(26) W. Schütze, "Über die Kohäsionsgrenzen synthetischer Kaliumhalogenidkristalle", Zeitschr. für Physik, Vol. 76, 1932, p. 135.

(27) R. Lad, "Crack Formation on NaCl Single Crystal Surfaces", Journal of Applied Physics, Vol. 23, 1952, p. 800.

(28) F. Seitz and T. Read, "Theory of the Plastic Properties of Solids", Journal of Applied Physics, Vol. 12, 1941, p. 482.

(29) J. Obreimow and L. Schubnikoff, "Über eine optische Methode zur Untersuchung von plastischen Deformationen in Steinsalz", Zeitschr. für Physik, Vol. 41, 1927, p. 907.

(30) S. Konobojewski and J. Mirer, "Innere Spannungen aus Asterismus bei Laue Bildern", Z. Kristallographie, Vol. 81, 1932, p. 69.

(31) A. Joffé, M. Kirpitschewa, and M. Lewitsky, "Joffé Effekt", Z. für Physik, Vol. 22, 1924, p. 286.

(32) P. Rehbinder, L. Schreiner, K. Zhigach, "Hardness Reducers in Drilling", Moscow, 1944 (Translated by the Council for Scientific and Industr. Research, Melbourne 1948).

(33) D. Harris, "Krypton Apparatus for Surface Area Measurements", Expiremt I-B", Metallurgical Dept., M.I.T.

(34) F. Wick and E. Carter, "Thermoluminescence Excited by High Voltage Cathode Rays", J. of the Optical Society of Am., Vol. 18, 1929, p. 387.

(35) B. Davis and W. Stempel, Physical Review, Vol. 17, 1921, p. 526.

(36) D. Rosenthal and M. Kaufman, "X-Ray Line Broadening of Plastically Deformed Marble", J. of Applied Physics, Vol. 23, 1952, p. 600.

(37) J. Peychè , "The Viscous Flow of Glass at Low Temperature", Soc. of Glass Technology, Journal, Vol. 36, 1952, p. 164.

(38) Ch. Palache, H. Berman, and C. Frondel, "Dana's System of Mineralogy, Vol. II", New York, 1951.

(39) E. R. Marshall and M. C. Shaw, "Forces in Dry Surface Grinding", Trans. ASME, 1952, p. 51.

(40) G. Masing
Zeitschr. für Metallkunde 1953

(41) P. Rehbinder, "Härte-abnahme bei Adsorbtion polarer Moleküle", Zeitschr. für Physik, Vol. 72, 1921, p. 191.

Appendix I

From Shaw (14), p.12-13:

Surface temperature $\theta = \text{const.} \times \frac{q.\ell}{k.\sqrt{L}}$ (Eq. 14)

where: $L = \frac{V.\ell}{2.K} = \frac{V.\ell.\rho.c}{2.k}$

and heat flow $q = \frac{u.V.d}{2.\ell}$ (Btu/in^2.sec)

u = grinding energy per unit volume
V = table speed of surface grinder
d = depth of cut
$2.\ell$ = total length of contact (compare Fig. 47)
ρ = specific weight
c = specific heat
k = coefficient of thermal conductivity

Combination of the 3 equations yields:

$$\theta = \text{const.} \times \frac{d.\sqrt{V}}{\sqrt{2.\ell}} \times \frac{u}{\sqrt{\rho.c.k}}$$

The second factor is constant for unchanged grinding geometry.

Thus we can simplify:

$$\theta = \text{const.} \times \frac{u}{\sqrt{\rho.c.k}}$$

This equation expresses the influence of varying material constants.

Appendix II

The vertical component of the temperature gradient

$\frac{\partial \theta}{\partial z} = \text{const.} \times \frac{q}{k}$ (The same equation can be obtained from fig.11 of (14), p.12-13)

$q = \frac{u.V.d}{2.\ell}$ (as in appendix I)

For simple geometrical reasons it follows for $2.\ell$:

$2.\ell \approx \sqrt{2.d.R}$, where R = radius of grinding wheel

Thus $\frac{\partial \theta}{\partial z} = \text{const.} \times \frac{u.V}{k} \sqrt{\frac{d}{R}}$

Appendix III

Calculated coefficient of thermal expansion α of marble (from (19) or (2o))

$$\alpha = \frac{2.\alpha_x(S_{33} - S_{13}) + \alpha_z(S_{11} + S_{12} - 2.S_{13})}{S_{11} + S_{12} - 4.S_{13} + 2.S_{33}}$$

The coefficients of compressibility S are taken from Schmid and Boas (11).

The coefficients α_x and α_z are taken from (11) or (2).

$$\alpha = \frac{-2x\ 5.4(17.5 + 4.3) + 26.21(11.3 - 3.74 + 2x4.33)}{11.3 - 3.74 + 4\ x4.33 + 17.5} \times 10^{-6}$$

$$\alpha = 3.17 \times 10^{-6}$$

Appendix IV

Microscopic thermal stresses (compare fig. 13) z-axis $\parallel$ c
x and y-axis $\perp$ c

$$\varepsilon - \alpha_z.t = S_{33}.\sigma_z = t.(\alpha - \alpha_z) \qquad \sigma_z = \frac{\alpha - \alpha_z}{S_{33}}.t$$

ε = thermal strain of marble vice
α = coefficient of thermal expansion of marble
α_x = coefficient of thermal expansion of calcite $\perp$ c
α_z = coefficient of thermal expansion of calcite $\parallel$ c
σ_x = stress in calcite column $\perp$ c
σ_z = stress in calcite column $\parallel$ c
t = temperature increase (°C)

$$\sigma_z = -\frac{(26.8 - 8.1)}{17.5} \times 10^7 \frac{\text{dynes}}{\text{cm}^2} \times t$$

$$\frac{\sigma_z}{t} = -145 \text{ PSI/°C}$$

Appendix V

Nomenclature as in appendix IV

$$\left|\begin{array}{l} \varepsilon - \alpha_x . t = (S_{11} + S_{12})\,\sigma_x + S_{13}\,\sigma_z = t(\alpha - \alpha_x) \\ \\ \varepsilon - \alpha_z . t = 2.S_{13}\cdot\sigma_x + S_{33}\cdot\sigma_z = t.(\alpha - \alpha_z) \end{array}\right|$$

(From (19), with $\sigma_x = \sigma_y$ and shear stresses = o)

$$2.\frac{S_{13}^2}{S_{33}} \cdot \sigma_x + S_{13}\cdot\sigma_z = \frac{S_{13}}{S_{33}}.t.(\alpha - \alpha_z)$$

$$(S_{11} + S_{12} - 2.\frac{S_{13}^2}{S_{33}})\cdot\sigma_x = t.(\alpha - \alpha_x - \frac{S_{13}}{S_{33}}.(\alpha - \alpha_z)$$

$$(S_{11}S_{33} + S_{12}S_{33} - 2.S_{13}^2)\,\sigma_x = t.\alpha.\left[(1 - \frac{\alpha_x}{\alpha}).S_{33} - S_{13}(1 - \frac{\alpha_z}{\alpha})\right]$$

$$\frac{\sigma_x}{t} = \alpha.\ \frac{S_{33}.(1 - \frac{\alpha_x}{\alpha}) - S_{13}(1 - \frac{\alpha_z}{\alpha})}{(S_{11}S_{33} + S_{12}S_{33} - 2.S_{13}^2)}$$

on the other hand:

$$\left|\begin{array}{l} -2.S_{13}\cdot(S_{11} + S_{12})\,\sigma_x - 2.S_{13}^2\,\sigma_z = -\alpha.t.(1 - \frac{\alpha_x}{\alpha}).2.S_{13} \\ \\ +2.S_{13}\cdot(S_{11} + S_{12})\,\sigma_x + S_{33}(S_{11} + S_{12})\,\sigma_z = \alpha.t.(1 - \frac{\alpha_z}{\alpha}).(S_{11} + S_{12}) \end{array}\right|$$

$$(S_{11}S_{33} + S_{12}S_{33} - 2.S_{13}^2)\,\sigma_z = t.\alpha\left[(S_{11} + S_{12}).(1 - \frac{\alpha_z}{\alpha}) - 2.S_{13}(1 - \frac{\alpha_x}{\alpha})\right]$$

$$\frac{\sigma_z}{t} = \alpha.\ \frac{(S_{11} + S_{12})(1 - \frac{\alpha_z}{\alpha}) - 2.S_{13}(1 - \frac{\alpha_x}{\alpha})}{(S_{11}S_{33} + S_{12}S_{33} - 2.S_{13}^2)}$$

Appendix V (Cont'd)

with $\alpha = 8.1 \times 10^{-6}$ (from (3) for Massachusetts Marble)

$$\left.\begin{aligned} \alpha_z &= +26.21 \times 10^{-6}/^{\circ}C \\ \alpha_x &= -\ 5.4 \times 10^{-6}/^{\circ}C \\ S_{11} &= +\ 11.3 \times 10^{-13}\ cm^2/dyn \\ S_{12} &= -\ 3.74 \times 10^{-13}\ cm^2/dyn \\ S_{13} &= -\ 4.33 \times 10^{-13}\ cm^2/dyn \\ S_{33} &= +\ 17.5 \times 10^{-13}\ cm^2/dyn \end{aligned}\right\} \text{ from (11)}$$

The equations derived on the preceeding page yield for

$$\underline{\underline{\frac{\sigma_x}{t}}} = +\ 5.29 \times 10^{6}\ dyn/cm^2 = 5.39\ kg/cm^2 = \underline{\underline{+\ 76.6\ PSI}}$$

$$\underline{\underline{\frac{\sigma_z}{t}}} = -\ 10.58 \times 10^{6}\ dyn/cm^2 = -\ 10.78\ kg/cm^2 = \underline{\underline{-\ 153\ PSI}}$$

With the corresponding coefficients for cadmium single crystals (11) and α as used by Laszlo (19):

$$\frac{\sigma_x}{t} = +\ 7.59 \times 10^{6}\ dyn/cm^2 = +\ 7.74\ kg/cm^2 = +\ 110.2\ PSI/^{\circ}C$$

$$\frac{\sigma_z}{t} = -\ 1.88 \times 10^{6}\ dyn/cm^2 = -\ 1.91\ kg/cm^2 = -\ 27.2\ PSI/^{\circ}C$$

These are the main stresses. The maximum shear stresses are:

$$\tau_{max.} = \frac{110.2 + 27.2}{2} = 68.7\ PSI/^{\circ}C$$

Laszlo found for the max. shear stress 71.3 PSI/°C for cadmium

Appendix VI

Maximum surface temperatures. Nomenclature as in app. I and II.

For depth of cut	$d = \frac{1}{2}.10^{-3}$	4.10^{-3} in.
$l = \frac{1}{2}\sqrt{2.d.R}$, (R = 3.5")	l = 0.042"	0.118"
$L = \frac{V.l}{2.K}$ V = 12.2 ft/min		
K = 0.0091 cm^2/sec (3),	L = 36.1	102.2
grinding energy per unit volume (measured)	$u = 3.8 \times 10^6$	1.7×10^6 in.lb/in^3
width of cut m = ¼"		
total grinding energy	= 31.3	112 cal/sec
heat flow	q = 232	293 cal/cm^2.sec
k = 0,00502 cal/sec.cm.°C,(3)		
$\theta_m = 1.13 \frac{q.l}{k.\sqrt{L}}$ ((14),p.12-13)	θ_m = 416 resp.	890 °C

These results have to be considered as approximations, since the thermal coefficients are not constant for temperature increases of this magnitude.